STRAIN RATE CHANGE EFFECT ON THE WORK HARDENING RATE IN TWO COMMERCIAL ALUMINIUM ALLOYS

S.R. Skjervold and S. Tjøtta
Hydro Aluminium a.s, R&D Centre, Karmøy, N-4265 Hävik, Norway

Abstract

In the present work, the effect of strain rate changes on elongation and strain localisation in the uniaxial tension of soft annealed AA3103 and solution heat treated AA6082 alloys was investigated. For the two alloys, the elongation up to maximum load was found to be similar, whereas the deformation in the post uniform region was different. The ability to distribute strain beyond the uniform elongation, and thereby delay the neck development, was found to be excellent for alloy AA3103. In this alloy it was posible to increase the uniform elongation by acelerating the testing rate. The uniform elongation was observed to increase with a factor of about 1.75 when the strain rate was increased with a factor of 10 just before the position of maximum load. This effect was found to be linked to a significant rate sensitivity of work hardening in the AA3103 alloy. The observed phenomenon is, however, strongly alloy dependent since the work hardening rate for an AA6082 alloy was not affected by acelerating the testing rate.

Introduction

An important forming limitation in thin walled aluminium sheets or extrusions is the occurrence of flow localisation (*necking*) during stretching. Local necks in uniaxial tension are a necessary consequence of a work hardening rate that decreases with increasing strain.
In uniaxial tension of aluminium, there has been observed a significant effect of strain rate on the true rate of work hardening when accelerating the testing rate [1,2]. This effect has been reported to increase significantly the post uniform elongation of AA3XXX and AA1XXX alloys compared to constant strain rate tests.
In the present work, the effect of accelerating deformation rates on the post uniform elongation in uniaxial tension of a soft annealed AA3103 and solution heat treated AA6082 alloy was investigated.

Experimental

The chemical composition of the two alloys studied (AA3103 and AA6082) are given in Table I.

Table I. Chemical composition of the two alloys (wt%).

Alloy	Si	Fe	Mg	Mn	Cu	Others	Al
AA3103	0.13	0.57	-	1.03	-	<0.05	Balance
AA6082	1.05	0.27	0.87	0.41	0.10	"	"

Specimens with the geometry shown in Fig. 1 were machined from aluminium extrusions with the tensile axes being parallel to the original extrusion direction. The tubes (AA3103) and the flat bars (AA6082) were tested according to the DIN-50140 and the DIN-50145 standards respectively. Tests were carried out using both constant and accelerating crosshead velocities. The three velocities used gave nominal strain rates of about 5.6×10^{-4}, 1.67×10^{-3} and 5.54×10^{-3} s^{-1}. The accelerating sequence was manually controlled, so that when the tensile load was judged to achieve the maximum value at the current rate, the crosshead velocity was increased by a factor of 10. In practice, this strain rate jump was made at a true strain of $\varepsilon=0.14$ and $\varepsilon=0.11$ for alloys AA3103 and AA6082 respectively.

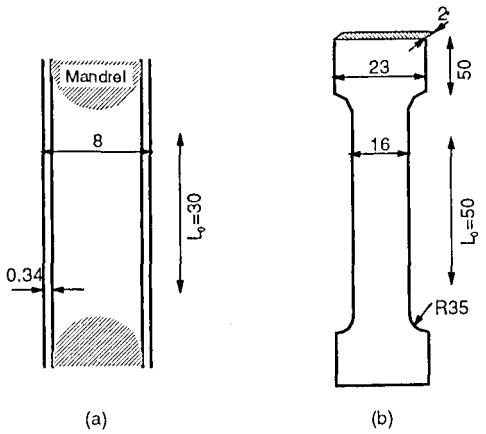

Figure 1. Sketch of the specimens used for tensile testing of (a) AA3103 tubes, and (b) AA6082 bars. The dimensions are given in mm.

The ABAQUS finite element code was used to analyse the evolution of stress state and strain rate during a tension test of the AA3103 tubes.

Results and Discussion

Typical load-elongation curves from uniaxial tensile tests at constant speed are shown in Fig. 2 for alloy AA3103 and AA6082 in the soft annealed and the solution heat treated condition respectively. As expected, the latter alloy obtain a much higher maximum load. The elongation to maximum load *(i.e. the uniform elongation-ε_u)* is almost equal for the two alloys, being ε_u=0.20 for AA3103 and ε_u=0.19 for AA6082. Beyond uniform elongation, in the so-called post-uniform region, the two alloys behaves quite differently again as the total elongation to fracture being much higher for the AA3103 alloy. The ability to distribute strain beyond uniform elongation, and thereby delay the neck development, is found to be much better for alloy AA3103. The post-uniform true strain was found to be ε=0.19 and ε=0.02 for AA3103 and AA6082 respectively.

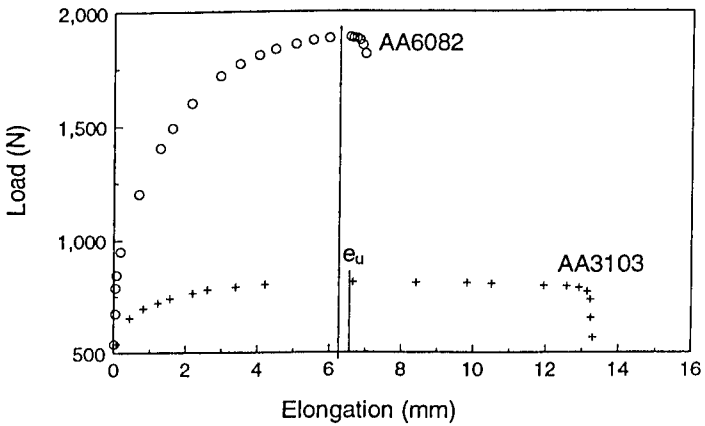

Figure 2. Load versus elongation for soft annealed AA3103 and solution heat treated AA6082 alloys. The curves are corrected for the difference in specimen geometry, (Fig. 1).

In Fig. 3a, the true stress - true strain curve for alloy AA3103 is represented by the Ludwik equation, $\sigma = \sigma_0 + K\varepsilon^n$, where σ_0 and K are the yield stress and the strength coefficient respectively. The experimental data was fitted to Ludwik's equation in the strain interval between ε=0.02 and ε_u, and the best fit were found by the least-square method. Parameters for alloy AA3103 were σ_0 = 41.7 MPa, K = 113.3 MPa and n = 0.29.

When using the Ludwik stress-strain curve in Fig. 3a in a finite element simulation of the tensile test, the total elongation was underestimated as seen in Fig. 3b. To obtain an excellent fit beyond uniform elongation a modified stress - strain curve was used, see Fig. 3a. This curve was simply obtained by adjusting the n-exponent to a higher value in the post-uniform interval so that the work hardening rate increases slightly with increasing elongation. However, this adjustment is rather unrealistic since all experimental observations show that the n-exponent decreases with increasing strain during standard tensile testing of aluminium alloys.

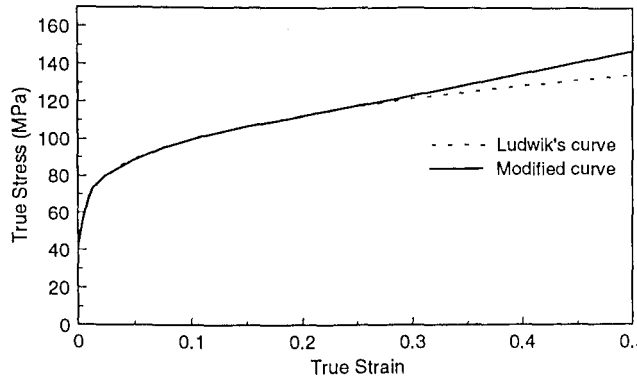

(a)

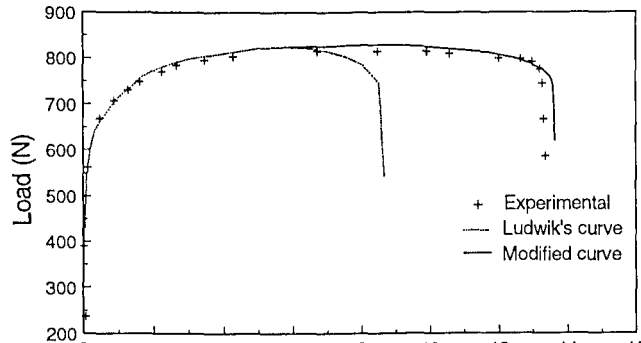

(b)

Figure 3. (a) True stress versus true strain using an extrapolated Ludwik's law and a modified curve for the AA3103 alloy. (b) Both curves used as input in FEM simulation of the tensile test.

To explain the observed effect of prolonged deformation beyond uniform elongation in alloy AA3103, and the apparent difference between the two alloys on Fig. 2, is thus not straightforward. There are three alternative hypothesis of this phenomenon;

a) *Anisotropic effects due to change from uniaxial to multiaxial state of stress in the necked region.*

b) *Positive strain rate sensitivity -m.*

c) *The strain hardening exponent -n increases with increasing strain rate*

The evolution of stress and strain rate during a tension test of the AA3103 tubes was simulated by using the finite element model (ABAQUS) mentioned above with the modified work hardening law. A magnification of the deformed element mesh in Fig. 4 shows the neck region. The simulation results clearly reveal a significant change in stress state (triaxiality) in the neck,

see Fig. 5a. As seen in Fig. 5a, the triaxiality of element no. 1 is equal to 0.333 during uniform deformation, whereas it exceeds 0.5 when diffuse or local necking occurs. Due to this change in stress state, hypothesis (a) can possibly explain the apparent increase in work hardening rate.

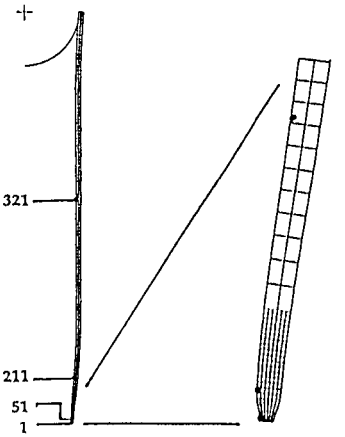

Figure 4. A magnified sketch of the deformed element mesh showing the development of a local neck in the tube wall.

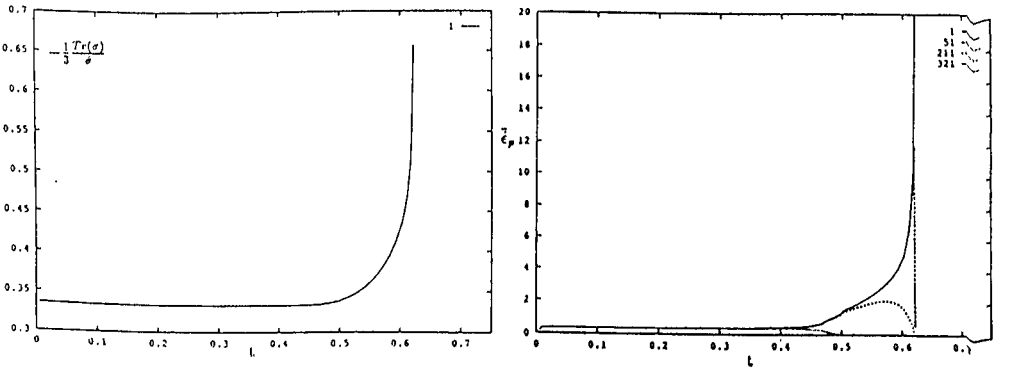

Figure 5. The development of triaxiality in position no. 1 (left) and the evolution of equivalent strain rate in four different positions (1, 51, 211 and 321) plotted versus time (right).

The evolution of equivalent strain rate is plotted in Fig. 5b for four different position, 1, 51, 211 and 321. In the uniform strain region the strain rate is constant and no difference is seen between the four positions. As the triaxiality starts to develop, *i.e. diffuse necking*, there is an accelerating strain rate in the necked region (position 1, 51 and 211), whereas the strain rate in position 321 outside the neck decreases to zero. The strain rate in position 211 reaches a plateau before it decreases to zero when the deformation become more localised in the final

stage of necking. In the necked region, position 1 and 51, the strain rate is seen to increase by several orders of magnitude. Since these materials have a positive strain rate sensitivity factor, m, this significant strain rate increase in the necked region can also be a possible explanation to the post uniform elongation.

In order to evaluate the effect of strain rate sensitivity, *hypothesis (b)*, on the flow stress, a number of accelerating strain rate tests were performed for both alloys. The accelerating strain rate test was selected instead of the monotonic test with various strain rates for two reasons; First, in an accelerating strain rate test of a single specimen the effect of material inconsistency is eliminated. Second, the effect of deformation structure on the strain rate sensitivity is included.

In the accelerating strain rate test the crosshead velocity was increased by a factor of 10 at a true strain of ε=0.14 and ε=0.11 for alloy AA3103 and AA6082 respectively. In addition, AA3103 was tested at three different initial strain rates to see if that affected the strain rate sensitivity. The strain rate sensitivity m can be expressed as $m = \Delta \ln \sigma / \Delta \ln \dot{\varepsilon}$ when the general relationship, $\sigma = (\sigma_0 + K\varepsilon^n)(\dot{\varepsilon})^m$ between flow stress and strain rate at constant temperature and strain is used.

In Table II, the m-factor is shown to be quite low, but positive, for both alloys. The m-factor is also shown to increase with increasing strain rate for alloy AA3103. At ε=0.5 the modified stress strain curve, Fig. 3a, is approx. 8% above the extrapolated Ludwik curve. In a material having a strain rate sensitivity of 0.006, an increased strain rate by a factor of 10 correspond to an increased flow stress of 1.5%. So although this positive strain rate sensitivity factor -m is closing the gap between Ludwik's flow curve and the modified one, there must be some additional effects which explains the deviation seen on Fig. 3a. This assumption is also supported by the evidence of having almost equal m-factors for the two alloys, see Table II.

Table II. Strain rate sensitivity factors (m) for AA3103 and AA6082 alloys tested at room temperature.

Alloy	$\dot{\varepsilon}$ =3.1 x10^{-3} s^{-1}	$\dot{\varepsilon}$ =9.2 x10^{-3} s^{-1}	$\dot{\varepsilon}$ =3.1 x10^{-2} s^{-1}
AA3103	0.0047	0.0056	0.0065
AA6082		0.005	

During the strain rate tests it was observed that the uniform elongation of AA3103 tubes was increased significantly in the strain rate jump test compared to the monotonic test. At constant strain rates it was measured an uniform true strain of ε_u=0.20, whereas in the accelerating strain rate tests, the uniform true strain was increased to about ε_u=0.35.

In Fig. 6, the true stress and the work hardening rate are plotted against true strain for alloy AA3103 in a test where the strain rate was increased from 5.6x10^{-4}s^{-1} to 5.5x10^{-3}s^{-1} at a true strain of 0.14. For comparison, the monotonic tension test fitted to the Ludwik equation is also shown. As can be seen, there is a significant effect of accelerating strain rate on the true rate of work hardening, and thereby an increase in uniform elongation. It also seems to be evident that the total elongation of tensile tests were not affected by accelerating strain rate to the same

extent as the uniform elongation. This is in accordance with findings reported recently by Bate on strain rate jump testing of Al-Mn alloys [3,4].

The AA6082 alloy did not exhibit the same effect of accelerating strain rate on the true rate of work hardening. The difference in specimen geometry used in the present work, see Fig. 1 , may give some variations in the development of necking. This geometrical effect is, however, assumed to be of minor importance which is confirmed by earlier work by Herø [1] on Al99.7 and Al-Mn alloys, and more recently by Date and Padmanabhan [2] on Al-Mn alloys again. In both of these works a significant effect of accelerating strain rate on the true rate of work hardening was found when using flat specimens with a varying thickness from 1 to 3 mm. The latter authors reported that the strain hardening exponent -n was increased from n=0.14 to n=0.27 when the strain rate was accelerated by a factor of 10. This is in good correspondence with the present findings where the strain hardening exponent -n was increased from n=0.20 to n=0.28 in the region before and after the strain rate jump respectively.

The low effect in AA6082 is then suggesting that the observed strain rate effect on the work hardening rate is alloy dependent, and thus controlled by some microstructural parameters which not are fully understood.

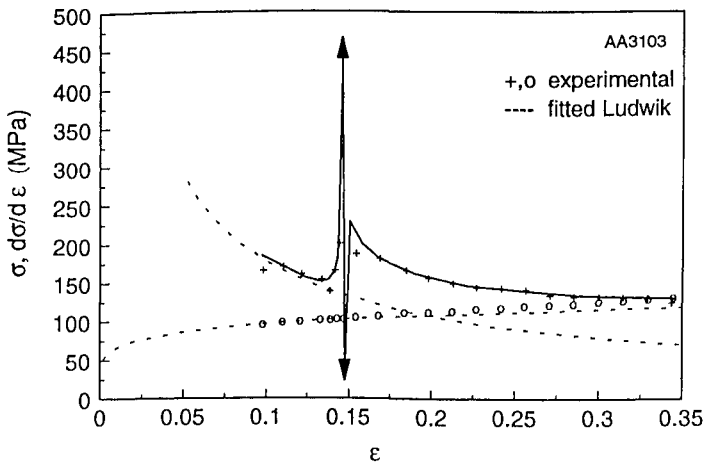

Figure 6. The true stress and work hardening rate plotted versus true strain showing the effect of a strain rate jump test of the AA3103 alloy. The strain rate was changed from 5.6 $x10^{-4}$ to 5.5 x 10^{-3} s^{-1} at a true strain of 0.14. The monotonic curve fitted to Ludwik's law is included for comparison.

Conclusions

In uniaxial tension of soft annealed AA3103 tubes the nominal uniform elongation was increased by a factor of 1.75 when the deformation speed was increased by a factor of 10 at a true strain of 0.14. This effect was found to be associated with a large strain rate sensitivity of work hardening.

A solution heat treated AA6082 alloy, tested under similar conditions, did not obtain an increased work hardening rate, and thereby increased formability.

Acknowledgements

The authors thank Prof. B. Anderson and M. Wilhelmsen at SINTEF for their contribution to this work.

References

1. H. Herø, Ph.D. thesis, Chalmers university of technology, Sweden (1978).
2. P.P. Date and K.A. Padmanabhan, Journal of Materials Processing Technology, 39, 153 (1993).
3. P.S. Bate, Met. Trans., 24A, 2679 (1993).
4. P.S. Bate, Met. Trans., 24A, 2691 (1993).